Supplementary materials:

Figure S1

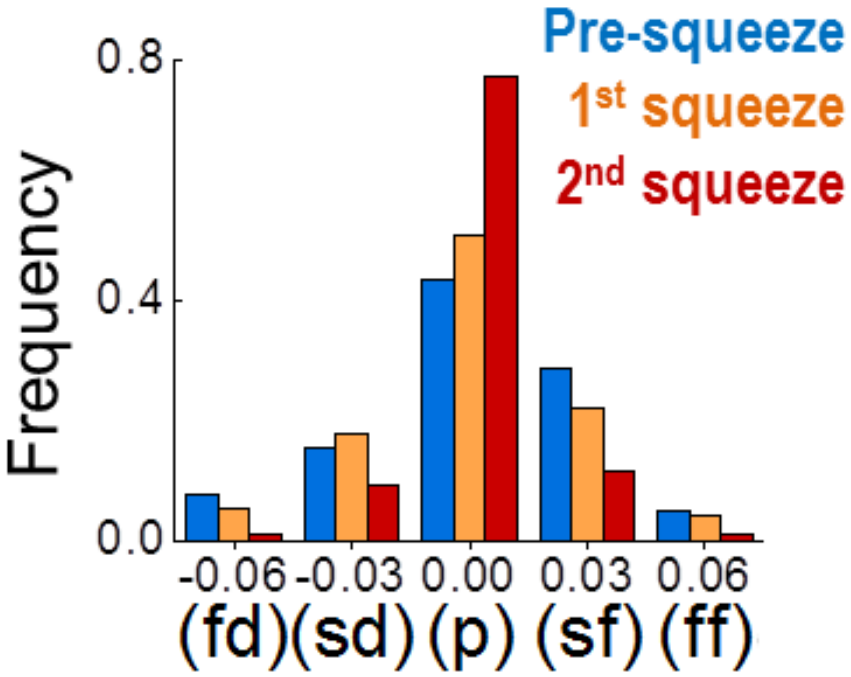

The growth rates at distinct levels of squeezing (Fig. 2C) are assembled in five bins that represent the different phases of clathrin-coated vesicle formation (fd, fast dissolution; sd, slow dissolution; p, plateau; sf, slow formation; ff, fast formation).

Figure S2

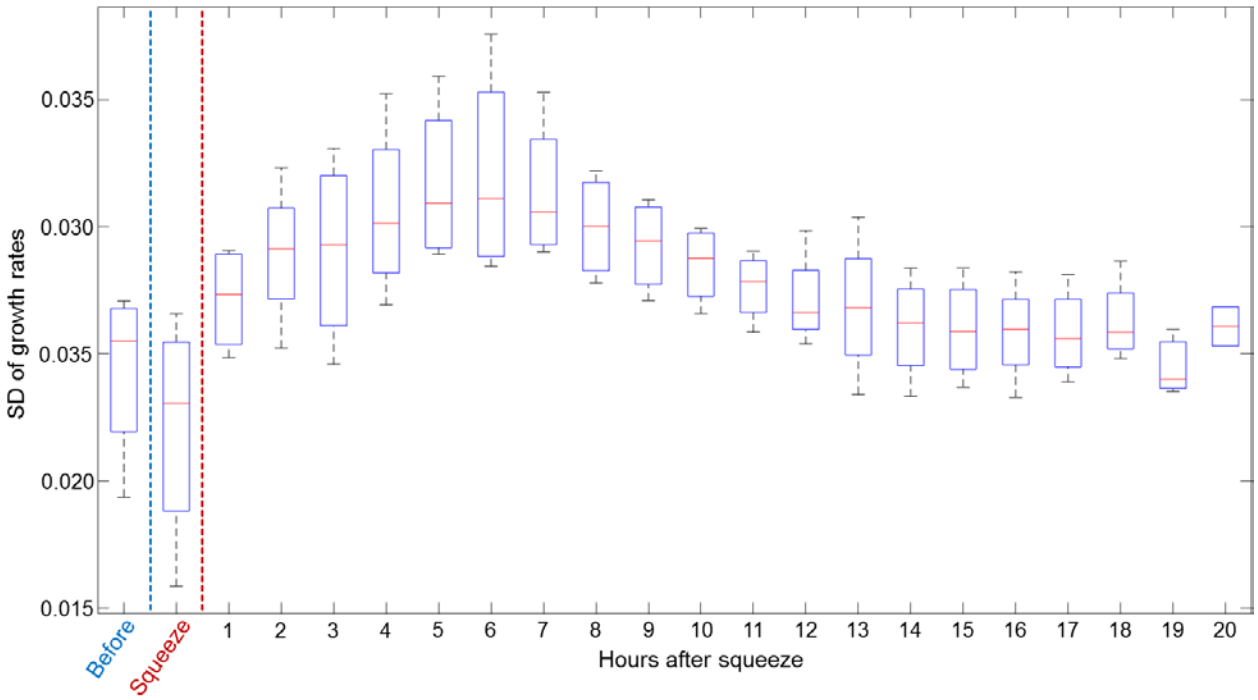

To verify the viability of BSC-1 cells after squeezing we monitored the clathrin coat activity for up to 20 hours. We imaged cells for 2 minutes in each hour to minimize photobleaching and phototoxicity. The box plots show the SD of clathrin coat growth rates determined at different time points (N_{cells} = 4, N_{traces} = 139678). The increased SD of growth rates after squeezing step signifies the retrieval of the endocytic dynamics in cells. Boxes extend to the quartiles, with a line at the median. Whiskers extend from the minimum to the maximum value.

Figure S3

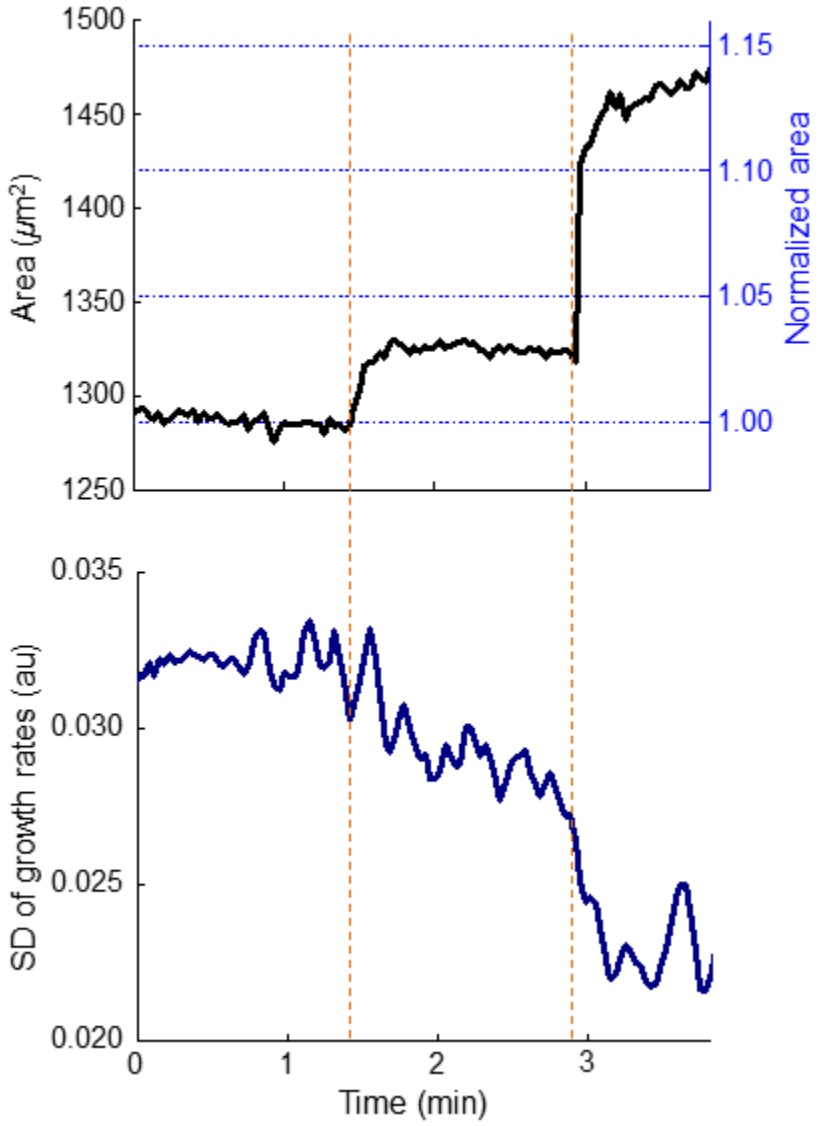

During development of the *Drosophila* wing imaginal disc, compression of the tissue changes the projected area of the center cells ~1.5 fold (Aegerter-Wilmsen et al., 2012). In our squeezing experiments, compressions that result in milder changes in the projected cell area produce observable changes in clathrin coat dynamics. The upper panel shows the change in the area of a BSC-1 cell during two squeezing steps (shown by the orange dashed lines). The axis on the right shows the cell area normalized to the average pre-squeeze level. The lower panel is the change in the SD of clathrin coat growth rates.

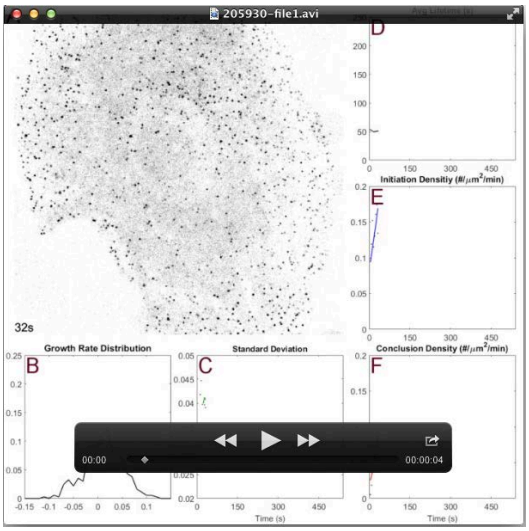

Movie 1. (A) Endocytic clathrin dynamics is imaged at the ventral surface of a BSC-1 cell during microaspiration (begins at *t*=180s). **(B)** Clathrin coat growth rate distributions are assembled for each time point of the movie. The distributions get more peaked as the clathrin coat dynamics slow down (Ferguson et al., 2016). **(C)** The standard deviation (SD) of the growth rate distributions (shown in B) is plotted against time. Also shown are the time variations of the average clathrin lifetime **(D)**, formation **(E)** and conclusion **(F)** densities.

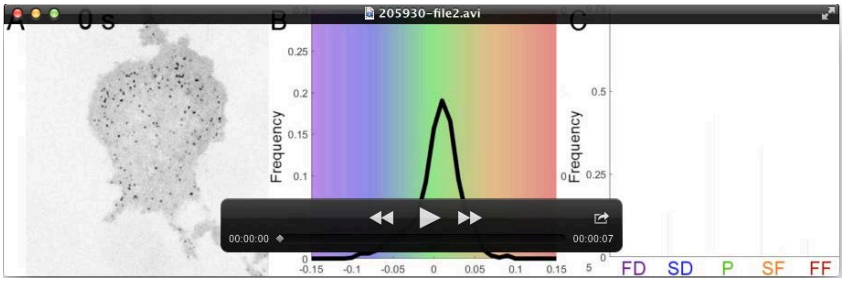

Movie 2. (A) Inverted movie shows clathrin dynamics at the ventral surface of a BSC-1 cell at different levels of squeezing. **(B)** Clathrin coat growth rate distributions are assembled for each time point of the movie. **(C)** Growth rate distributions are shown as bar plots, where each bin represents a different growth phase (FD, fast dissolution; SD, slow dissolution; P, plateau; SF, slow formation; FF, fast formation)(Ferguson et al., 2016). Squeezing steps can be observed as stepwise changes in the growth phases. Note that the high magnitude growth rates (FD & FF) diminish as the P phase gets more occupied with the increasing membrane tension.

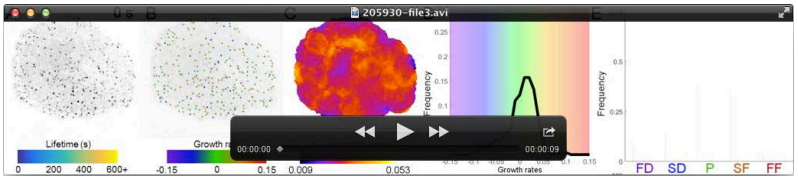

Movie 3. Clathrin coats are imaged at the ventral surface of a BSC-1 cell at different levels of squeezing and relaxation. Note that the dynamics is retrieved when the squeezing is withdrawn. **(A)** The traces of individual clathrin-coated structures are colored according to the lifetime. **(B)** Each clathrin coat is colored according to its instantaneous growth rate. **(C)** For each frame of the movie, SD maps are created by giving each pixel the value of the SD of the clathrin coat growth rates detected in a radius of 4.8 μm. **(D)** Clathrin coat growth rate distributions are assembled for each frame of the movie. **(E)** Growth rate distributions in (D) are shown as bar plots representing different growth rates.

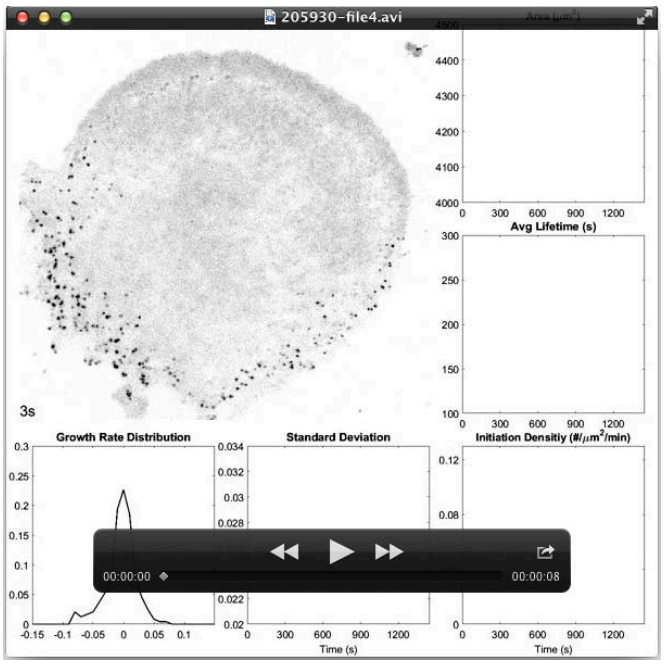

Movie 4. Movie shows clathrin coats at the ventral surface of a migrating astrocyte. The lamella extends towards the top-right corner of the image. Plots show the clathrin coat growth rate distributions, the SD of growth rate distributions, the area of the cell, average clathrin coat lifetime and initiation density of clathrin-coated structures. The arrow appearing at t = 177s marks the poking of the lamella by a micromanipulator controlled glass tip. The lamella starts to retract subsequently (see the change in the cell area). Note the increased number/density of clathrin-coated structures associated with the retraction.

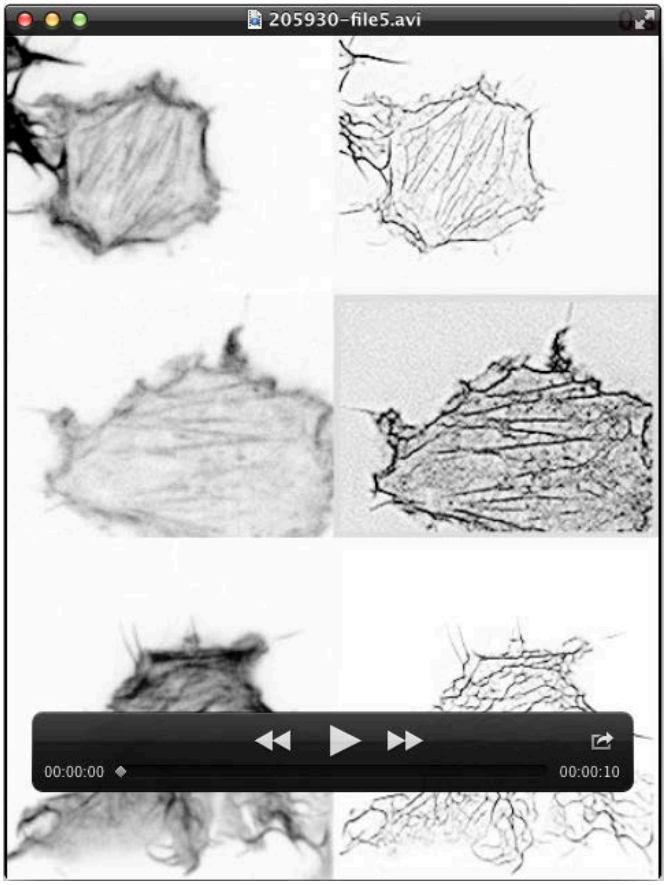

Movie 5. BSC-1 cells transiently expressing Lifeact-mCherry are subjected to squeezing starting from t = 180s (left). The right panel shows the super-resolution radial fluctuations (SRRF) reconstruction of the Lifeact signal (Gustafsson et al., 2016). The integrity of the actin cytoskeleton can be observed in both the conventional and super-resolved channels. Note the dynamic actin punctae appearing at the ventral surface of the cells.

References:

Aegerter-Wilmsen, T., Heimlicher, M. B., Smith, A. C., de Reuille, P. B., Smith, R. S., Aegerter, C. M., Basler, K., Adler, P. N., Charlton, J., Liu, J., et al. (2012). Integrating force-sensing and signaling pathways in a model for the regulation of wing imaginal disc size. *Development* **139**, 3221–31.

Ferguson, J. P., Willy, N. M., Heidotting, S. P., Huber, S. D., Webber, M. J. and Kural, C. (2016). Deciphering dynamics of clathrin-mediated endocytosis in a living organism. *J. Cell Biol.* **214**, 347–58.

Gustafsson, N., Culley, S., Ashdown, G., Owen, D. M., Pereira, P. M. and Henriques, R. (2016). Fast live-cell conventional fluorophore nanoscopy with ImageJ through super-resolution radial fluctuations. *Nat. Commun.* **7**, 12471.